D.V. GAMOV, O.I. GUDYMENKO, V.P. KLADKO, V.G. LITOVCHENKO,
V.P. MELNIK, O.S. OBEREMOK, V.G. POPOV, YU.O. POLISHCHUK,
B.M. ROMANIUK, V.V. CHERNENKO, V.M. NASEKA

V.E. Lashkaryov Institute of Semiconductor Physics, Nat. Acad. of Sci. of Ukraine
(41, Prosp. Nauky, Kyiv 03028, Ukraine; e-mail: romb@isp.kiev.ua)

RESEARCH OF RECOMBINATION CHARACTERISTICS OF Cz-Si iMPLANTED WITH IRON IONS

A comparative study of the defect formation and changes in the lifetime of nonequilibrium minority charge carriers in silicon while gettering the iron impurity with the use of a combined getter "porous silicon layer + aluminum film" is carried out. It is shown that, while annealing specimens with no getter layer, iron silicide and defects of the vacancy type are formed in the implanted regions and, as a result, a considerable reduction in the lifetime of nonequilibrium minority charge carriers is observed. The influence of the getter layer on the defect formation and the redistribution of iron atoms implanted into silicon are studied in the case of high iron concentrations in a vicinity of the surface. The presence of a getter layer is shown to reduce the efficiency of the silicide formation in the implanted region and to increase the concentration of interstitial defects in silicon. A model of the gettering process is proposed, which makes allowance for the gettering-induced reduction of the iron atom concentration in the implanted region and a decrease of the vacancy defect concentration, as well as the simultaneous increase of the concentration of interstitial-type defects associated with the formation of complexes of iron and boron atoms. These complexes are recombination-active and do not allow the lifetime of charge carriers to be restored to the initial value.

K e y w o r d s: silicon, gettering, iron, defects, lifetime, X-ray diffraction, mass spectrometry.

1. Introduction

The negative role of transition metal atoms in silicon used for manufacturing the photoconverters of the solar energy is associated first of all with the fact that heavy metal atoms, their precipitates, complexes with point defects, and impurities form deep centers in the band gap of silicon and, therefore, substantially reduce the lifetime of nonequilibrium minority charge carriers and, accordingly, the efficiency of the photoconversion process. High values of diffusion coefficient in silicon for those impurities result in that Si wafers become quickly contaminated even if point-like sources of metal ions are used and already at low-temperature treatments.

Recently, a special attention has been paid to studying the influence of the iron impurity [1], which can get to silicon at every stage of the technologi-cal process aimed at the fabrication of silicon and silicon-based photoconverters, because iron forms the basis of modern technological facilities. Iron can exist in silicon in the interstitial state, in the form of $FeSi_2$ silicide inclusions, or in the form of FeB complexes. In the interstitial state, iron forms a deep level with an energy position of $E_v + 0.38$ eV and capture cross-sections of 5×10^{-14} cm^{-2} for electrons and 7×10^{-17} cm^{-2} for holes [2]. Two levels, at $E_v + 0.1$ eV and $E_c - 0.26$ eV, emerge at the formation of FeB complexes [3]. It should be noted that FeB complexes can decay at low temperatures and under illumination, which makes the parameters of solar cells unstable [4].

Iron can create complexes with other metal impurities as well. It is known that iron participates in the formation of about 20 types of deep levels in silicon [5, 6]. The presence of iron with a concentration higher than 5×10^{11} cm^{-3} in photoconverters of the solar energy on the basis of single- and polycrystalline (multicrystalline) silicon also gives rise to a decrease of the photocell efficiency by 3 to 5% with respect to the initial values [7].

A harmful factor is the accumulation of iron at grain boundaries in polycrystalline silicon, which results in the short circuit of photocells. Iron is accumulated in defect regions and around SiO_2 precipitates. As a rule, this gives rise to a reduction of the open-circuit voltage in photoconverters. To reduce the impurity concentration in silicon, the method of gettering is used. It consists in the formation of a getter layer, in which the solubility of the Fe impurity exceeds that in silicon by orders of magnitude. The procedure itself includes the creation of a porous silicon layer [8], a silicon layer heavily doped with phosphorus [9], or a layer of AlSi eutectics [10] on the wafer rear side. To increase the efficiency of gettering, both the optimum gettering technique and the gettering annealing temperature must be selected; it should done to provide the maximal coefficient of impurity diffusion and the maximal coefficient of impurity segregation in the getter region.

In work [11], we showed the efficiency of application of a combined getter "porous silicon layer + Al layer" for the removal of recombination-active impurities from the bulk of multicrystalline Si. In that work, we studied the gettering mechanism of iron atoms implanted into single-crystalline silicon. The application of the ion implantation allows a controllable number of iron atoms to be introduced into silicon to a required depth, which is important for model experiments. This work was aimed at studying the recombination characteristics of silicon implanted with iron ions at its gettering onto the rear side of the wafers. The specific feature of the work consists in researching the influence of the getter layer on the processes of defect formation in the implanted region and the redistribution of iron atoms in the case of their high concentration (oversaturation).

2. Experimental Techniques and Specimens

Specimens (wafers) of single-crystalline silicon KDB-2 (100) grown up using the Czochralski method and doped with boron were studied. The impurity concentration in the examined specimens was measured using the glow discharge mass spectrometry. The measurements were carried out with the help of an "Element GD" device.

The background concentrations of actual recombination-active impurities in initial Si wafers were as follws: 5×10^{13} cm^{-3} for V, 1×10^{14} cm^{-3} for Cr, 1×10^{15} cm^{-3} for Mn, 2×10^{15} cm^{-3} for Fe, 2×10^{14} cm^{-3} for Ni, 1×10^{15} cm^{-3} for Cu, and 5×10^{13} cm^{-3} for Au. As was shown in work [12], after technological operations (annealing, formation of $p - n$ transitions, metallization, and so on), the concentrations of some impurities–mainly, iron–in silicon wafers essentially increased.

The working surface of a silicon wafer was implanted with the iron isotope ^{54}Fe (an implantation energy of 140 keV and an implantation dose of 2.4×10^{13} cm^{-2}). The isotope Fe^{54} was used to resolve the mass spectra of Fe and ^{28}Si$_2$. The getter layer was formed on the rear surface of a wafer. It consisted of a layer of porous silicon (por-Si) 3 μm in thickness and an aluminum film 2.4 μm in thickness. To provide the gettering of impurities, both implanted and background, the specimens were annealed in the argon atmosphere at temperatures of 800 or 900 °C for 30 min.

The profiles of impurity distributions over the depth of silicon structures were studied using the method of secondary ion mass spectrometry. The measurements were carried out on an ion microprobe mass spectrometer Atomica-6500. The diffusion length $L_D = (D\tau)^{1/2}$, where D is the diffusion coefficient of minority charge carriers, and τ the bulk lifetime of nonequilibrium charge carriers, was determined from the spectral dependences of surface photo-emf V_{ph} [13].

Information concerning the type, size, and concentration of structural defects in the studied silicon specimens was obtained by applying the technique of measuring the halfwidth of diffraction reflection curves (DRCs) and the method of X-ray diffuse scattering (XDS) [14–16]. The CuK$_{\alpha 1}$ radiation (the wavelength $\lambda = 0.15406$ nm, symmetric reflections 004) was used. The diffusion scattering and the DRCs were measured with the help of a high-resolution x-ray diffractometer "X'Pert PRO MRD". The measurements were carried out in a vicinity of the reciprocal lattice node 004. The XDS method allows one to reveal not only precipitates of a new phase and impurities, but also microdefects, in particular, point defect clusters (they cannot be detected using the electron microscopy), which are coherent with the matrix and characterized by diffused boundaries and small gradients of shift fields. This method also enables the microdefect type (vacancy or interstitial) to be distinguished, because the asymmetric part of
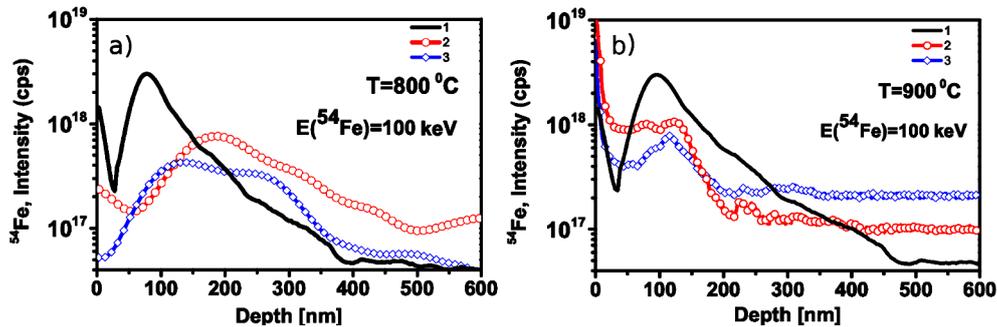
Fig. 1. Distribution profiles of the implanted ^{54}Fe impurity for the initial specimen (*1*) and for specimens annealed (2) without and (*3*) with the getter layer "porous Si + Al" on the rear side of a wafer after the annealing at $T = 800$ (*a*) and 900 °C (*b*)

XDS spectra shifts the scattering from defects of different types into different directions with respect to the reciprocal lattice node [16, 17]. In such a manner, we could not only observe defects, but also classify them by type and dimensions.

3. Experimental Results

In Fig. 1, *a*, the profiles of the implanted ^{54}Fe impurity distribution are shown for specimens implanted with iron, both without the getter layer "por Si + Al" and with it; the specimens were annealed at a temperature of 800 °C. The distribution of the iron impurity in the initial specimen has a maximum at the 85-nm depth. The accumulation of iron on the surface is also observed. When the specimens without the getter layer have been annealed, a redistribution of the iron impurity, namely a substantial reduction of the iron concentration at the maximum, takes place.

One can see that, in the specimen without the getter layer, the iron impurity becomes effectively redistributed, mainly into the specimen depth. In the presence of a getter layer, the iron impurity is accumulated less effectively on the specimen surface, and the distribution profile has a maximum at a depth of 130 nm; the concentration of iron at the distribution maximum becomes much lower than that in the specimens annealed without the getter; and, at the depth more than 550 nm, the iron concentration becomes lower than the device sensitivity, which testifies to the effective iron gettering. For instance, at a depth of 450 nm, the concentration of iron in the specimens without the getter layer is by almost an order of magnitude higher than the concentration obtained in the case where the specimens with the getter layer were annealed.

In Fig. 1, *b*, the profiles of the iron impurity distribution in the specimens with and without the getter layer "por-Si + Al" obtained before and after the annealing at a temperature of 900 °C are exhibited. The specimens with the getter layer demonstrate a "tail" with a uniform distribution of iron in the interval of depths where the analysis was carried out. The iron concentration in the interval from 200 to 600 nm is higher for the specimens with the getter layer.

The results of researches concerning the evolution of clusters of point microdefects are depicted in Fig. 2. Here, the distributions of the XDS intensity in the direction parallel to the reciprocal lattice vector (the q_z-cross-section, Fig. 2, *a*) and perpendicularly to it (the q_x-cross-section, Fig. 2, *b*) are shown for an implanted specimen (curve *1*) and for specimens without the getter layer (curve *2*) and with it (curve *3*) after their annealing at $T = 800$ °C; **q** is a vector that determines the distance from the reciprocal lattice node to the point of intensity measurement. First, let us consider the distribution of the XDS intensity for the implanted specimen (Fig. 2, *a*, curve *1*). The analysis of the curve shows that the specimen contains microdefects of both the vacancy (they ary responsible for the intensity at $q_x < 0$) and interstitial (the intensity at $q_x > 0$) types.

For the annealed specimen without the getter layer, the picture of the XDRS intensity distribution changes considerably for both cross-sections at the reciprocal lattice node (Figs. 2, *a* and *b*, curves *2*). At the q_z-cross-section, the intensity decreases in the interval $q_z < 0$ (at small q_z's) in comparison with that for the implanted unannealed specimen and practically vanishes at $q_z > 0$. At the same time, the intensity at the q_x-cross-section considerably grows. For
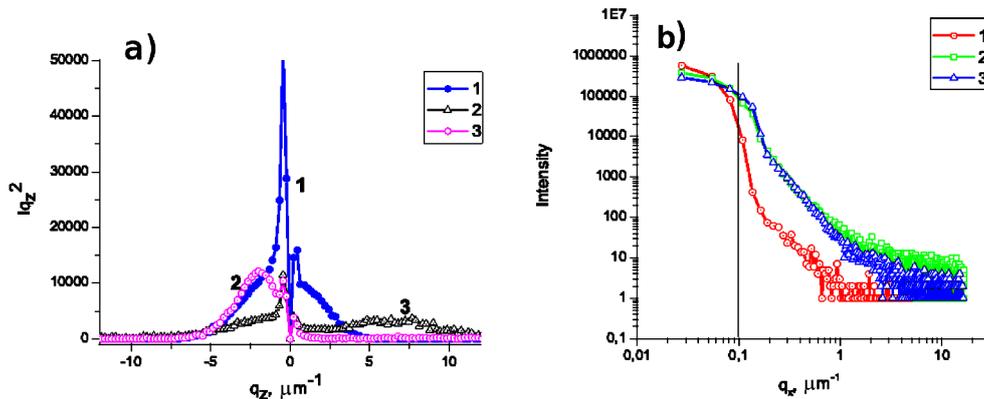
Fig. 2. Distributions of the XDS intensity in the directions (*a*) parallel to the reciprocal lattice vector (the q_z-cross-section) and (*b*) perpendicular to it (the q_x-cross-section, Fig. 2,*b*): (*1*) after the iron implantation, after the annealing of an implanted specimen (*2*) without and (*3*) with the getter layer
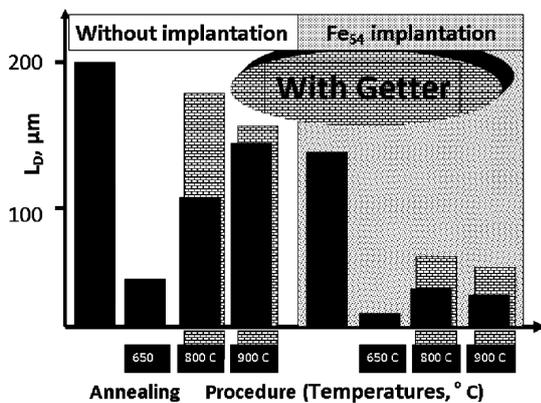

Fig. 3. Dependences of the diffusion lengths of nonequilibrium minority charge carriers, L_D, on the annealing temperature for the initial specimens after the annealing and the specimens doped with iron atoms without and with the getter layer. The parameters of treatments are indicated in the figure

the annealed specimen with the getter layer, the XDS intensity distribution changes for both node cross-sections (Figs. 2, *a* and *b*, curves *3*). At the q_z-cross-section, the intensity decreases at $q_z < 0$ in comparison with that for the annealed specimen without the getter layer and strongly grew at $q_z > 0$ in the interval of large and small q_z-values.

In Fig. 3, the dependences of the diffusion length of nonequilibrium minority charge carriers, L_D, on the annealing temperature are shown for the initial specimens and the specimens doped with iron atoms, with and without the getter layer. The low-temperature annealing substantially reduces the initial value of

diffusion length. This fact can be associated with the formation of complexes "impurity–defect" with an enhanced recombination activity, as well as with the contamination of the specimen in the course of annealing. The application of aluminum getter allows the initial L_D-value to be partially restored. The combined getter "porous silicon + Al" is more effective: it practically restores the L_D-value of the initial material. The implantation of the iron impurity to a still higher concentration followed by the annealing considerably reduces the value of L_D. In this case, gettering also improves the quantity L_D, although to a less extent. The combined getter is much more effective than the aluminum one, as it was in the case of a polycrystalline material [11].

4. Discussion of the Results

According to the results of mass-spectrometry researches (Fig. 1), iron atoms implanted into the silicon wafer are located in a thin (of about 200 nm) layer, with a considerable part of the iron impurity being accumulated near the surface. The average concentration of iron in this layer amounts to 3×10^{18} cm^{-3}. If this number of iron atoms were uniformly distributed across a silicon plate 300 μm in thickness, their average concentration would reach 10^{16} cm^{-3}. This value considerably exceeds the equilibrium solubility of iron in silicon at the gettering temperature (10^{15} cm^{-3} at 800 °C). (Such high iron concentrations worsen the gettering conditions, but the sensitivity of the applied mass-spectrometry methods did not allow us to use lower iron concentra-

tions.) At the following annealing, some iron atoms diffuse deeply into the wafer. Since the diffusion coefficient of iron is rather high (of about 10^{-6} cm^2/s at 800 °C), iron atoms can diffuse across the whole wafer within several minutes. In the course of annealing, if the getter layer is absent, iron atoms form a silicide layer in the region of maximum accumulation of interstitial silicon atoms, whereas some Fe atoms become uniformly distributed across the silicon wafer with a concentration close to the solubility threshold at annealing temperatures. When the wafer is cooled down, iron atoms form complexes with the boron impurity or stay at the interstitial sites. At higher annealing temperatures, the equilibrium solubility of iron in Si increases, and the coefficient of segregation with respect to the getter decreases, so that the gettering efficiency diminishes. At the same time, when cooling down the wafers annealed at higher temperatures, much more iron atoms create complexes with boron atoms, which is confirmed by the results of mass-spectrometry researches (Fig. 1, *b*, curve *3*). This process considerably reduces the lifetime of charge carriers, which is testified by the experiments mentioned above (Fig. 3); see also the data on the getter annealing of multicrystalline silicon [18]. When the specimens with the getter layer are annealed, iron atoms are captured into the getter layer, so that there emerges a gradient of the Fe concentration in the wafer toward the getter, which provides the flux of iron atoms to the latter (Fig. 4).

Atoms of Fe enter the wafer bulk from the implanted layer as silicides decay. If the wafer contains SiO$_2$ microprecipitates with an excess concentration of interstitial Si atoms around them [19], iron atoms can form silicides in a vicinity of SiO$_2$ precipitates by engaging interstitial atoms, thus promoting a subsequent growth of the SiO$_2$ phase. This scenario is evidenced by the presence of interstitial-type defects, which are registered in the x-ray diffraction spectra (Fig. 2, curve *3*).

Let us consider the defect formation processes in the wafers after the implantation and the annealing in more details. From Fig. 2, *a*, one can see that the magnitude of reduced intensity, $I(q)q^{-2}$, is almost constant for various q. This means that $I(q) \sim q^{-3}$, which, in view of the specific character of measurements on a three-crystal diffractometer [15], corresponds to the so-called asymptotic region, when the microdefect (MD) power satisfies the condition
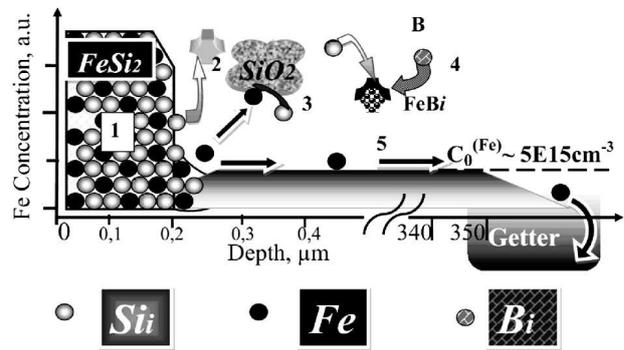

Fig. 4. Schematic illustration of the gettering process

$qS > (QC)^{-1/2}$, where Q is the scattering vector, and C is the MD power, which characterizes the volume variation induced by the defect, i.e. when the matrix is substituted by a MD. Since the transition to the horizontal section occurs at rather small deviations from the reciprocal lattice node, it is evident that, according to the position of the inflection point at $q \gtrless 0$, the MD dimensions are rather large; for example, the MD radius amounts to 0.08 μm for MDs of the vacancy type and to 0.12 μm for MDs of the interstitial type. The XDRS intensity is somewhat higher at negative q. Accordingly, the total volume of big vacancy-type MDs is somewhat larger (by 10%) than that of interstitial ones, because the XDRS intensity is proportional to the volume of defects. A rather low intensity at the q_x-cross-sections of the reciprocal lattice node for the implanted specimen (Fig. 2, *b*, curve *1*) testifies that MDs are defects with the spherical symmetry of displacement fields. Since the slope of the curve at $q_x > 0.1$ μm^{-1} is larger than 2, which corresponds to the asymptotic scattering, it is evident that a certain distribution of MDs over their dimensions takes place (the XDS intensity at $q_x < 0.1$ μm^{-1} is determined by the device tool function). The slope corresponding to the Huang scattering can be equal to 1 for some fraction of small defects and to 3 for the other (which corresponds to the asymptotic scattering). As a result, we obtain an intermediate value.

Microdefects in the annealed specimen without the getter layer acquire a nonspherical symmetry, which is evidenced by the distribution of the XDS intensity (Fig. 2, *a*, curve *2*). Since the XDS intensity falls down at $q_z < 0$, this gives us ground to assume that the number of vacancy-type MDs with large characteristic dimensions decreases, and the number of defects with dimensions less than 0.15 μm grows, which

confirms the formation of $FeSi_2$ silicide inclusions in the region of implanted iron distribution. There also emerge MDs of the interstitial type with small dimensions of 1 μm, and their concentration is lower in comparison with that in the implanted specimen not subjected to annealing.

For the specimen with the getter layer, the distribution of the XDS intensity changed for both node cross-sections (Figs. 2, *a* and *b*, curves *3*). At the q_z-cross-section, the intensity decreases at $q_z < 0$ in comparison with that for the specimen without the getter and strongly grows at $q_z > 0$ in the ranges of large and small q_z-values. Since the XDS intensity drops down at $q_z < 0$, we may assume that the number of vacancy-type MDs with characteristic dimensions of 0.05 μm decreases. Simultaneously, the intensity at the q_x-cross-section also increases considerably in the interval of large q-values. This fact testifies to the growth in the number of interstitial-type MDs with dimensions of 0.06 and 0.04 μm.

In Table, the concentrations and the average sizes of defects of the vacancy and interstitial types are quoted for the implanted and annealed specimens, which were determined from the distribution curves of the XDS intensity. The analysis of those results shows that, after the implantation into silicon, there emerge defects of both the vacancy and interstitial types with small dimensions and a high concentration. Those defects are associated with point defects generated at the implantation and with introduced iron atoms. Annealing gives rise to a reduction in the concentration and an increase in the dimensions of defects owing to the formation of silicides (the growth of the vacancy defect concentration) and the growth of interstitial defect complexes. In the specimens with the getter layer, the concentration of vacancy defects decreases owing to the iron gettering and, accordingly, the reduction in the number of $FeSi_2$ silicide inclu-

Concentrations and average sizes of defects of the vacancy and interstitial types

Specimen type	R_V, μm	C_V, cm^{-3}	R_I, μm	C_I, cm^{-3}
Implanted $^{54}Fe^+$	0.08	1.0×10^9	0.12	4×10^7
Implantation + Annealing (without the getter layer)	0.15	2.5×10^7	1	3×10^6
Implantation + Annealing (with the getter layer)	0.05	1×10^7	0.04	1×10^8

sions. The concentration of interstitial-type defects with small dimensions substantially increases, which can be connected with the iron diffusion toward the getter layer, some part of which creates FeB_i complexes in the bulk of a Si wafer.

At last, let us discuss the model of gettering the iron atoms implanted into silicon, provided that the getter layer is on the rear side of the wafer, which was described above (see Fig. 4). At the initial stages of the annealing of a specimen, $FeSi_2$ iron silicides intensively grow in the implanted layer (*1*), with some fraction of iron atoms, which have not reacted and formed silicides, diffusing into the depth of a Si wafer (*5*). Redundant interstitial atoms of silicon located in a vicinity of the "implanted layer–single crystal" interface create interstitial complexes in the course of annealing (*2*). If internal SiO_2 precipitates are present, iron atoms are partially captured by them and become excluded from the diffusion process (*3*). Iron atoms are effectively captured by the getter layer (the coefficient of segregation for the getter layer has an order of 10^{-5}). As a result, there emerges a gradient of the iron atom distribution across the wafer, which promotes the flux of iron atoms toward the getter layer. If the annealed specimens are cooled down, some iron atoms can form recombination-active complexes FeB_i in the bulk of the Si wafer (*4*), which gives rise to a reduction of the lifetime of nonequilibrium charge carriers. The presence of interstitial Si atoms, especially around SiO_2 precipitates, promotes the formation of silicides in the wafer bulk in the course of gettering. Respectively, the flux of iron atoms toward the getter decreases and weakens the action of the latter. Therefore, the gettering of iron in silicon is a complicated process that includes the diffusion of Fe atoms, formation of $FeSi_2$ silicides and FeB_i complexes, and interaction of iron atoms with internal SiO_2 precipitates. For weakening this harmful effect, thermal treatments promoting the decay of SiO_2 precipitates in the silicon bulk can be recommended.

5. Conclusions

It is shown that, when iron-implanted silicon specimens without the getter are annealed, iron silicide is formed in the implanted region, defects of the vacancy type emerge, and the lifetime of nonequilibrium minority charge carriers considerably decreases. The presence of the getter layer gives rise to a par-

tial restoration of the charge carrier lifetime. The influence of the getter layer on the processes of defect formation and redistribution of iron atoms implanted into silicon is studied in the case of high iron concentrations in the near-surface region. The presence of the getter layer is shown to reduce the efficiency of the silicide formation in the implanted region and to increase the concentration of interstitial defects in silicon, which are connected with the formation of complexes of iron and boron atoms. These complexes are recombination-active and do not allow the lifetime to be restored to the initial value. It is shown that the efficiency of gettering by a combined getter "porous Si + Al" is considerably higher than the gettering with the use of an aluminum film. In order to enhance the efficiency of gettering and to make the lifetime of charge carriers longer, the formation of complexes with iron must be eliminates, e.g., using a fast annealing and definite impurities that suppress the growth of SiO_2 precipitates.

1. A.A. Istratov, H. Hieslmair, and E.R. Weber, Appl. Phys. A **70**, 489 (2000).
2. D. Macdonald and L. Geerligs, Appl. Phys. Lett. **85**, 4061 (2004).
3. K. Schmalz, F. Kirscht, S. Nieze *et al.*, Phys. Status Solidi A **100**, 69 (1987).
4. G. Zoth and W. Berholz, J. Appl. Phys, **67**, 676 (1990).
5. A.A. Istratov, H. Hieslmair, and E.R. Weber, Appl. Phys. **69**, 13 (1999).
6. K.D. Glinchuk and N.M. Litovchenko, Optoelektron. Poluprovodn. Tekhn. Obzory **21**, 47 (1991).
7. V. Vahanissi, A. Haarahiltunen, H. Talvitie, M. Yli-Koski, and H. Savin, Prog. Photovolt. Res. Appl., DOI: 10.1002/pip.2215 (2012).
8. A.A. Evtukh, V.G. Litovchenko, A.S. Oberemok *et al.*, Semicond. Phys. Quant. Electr. Optoelectr. **4**, 278 (2001).
9. T.E. Seidel, R.L. Meek, and A.G. Cullis, J. Appl. Phys. **46** (1975).
10. S.M. Joshi, U.M. Gosele, and T.Y. Tan, J. Appl. Phys. **77**, 3858 (1995).
11. S.G. Volkov, A.A. Evtukh, V.G. Litovchenko *et al.*, Ukr. Fiz. Zh. **47**, 684 (2002).
12. V.G. Litovchenko, B.M. Romanyuk, V.G. Popov *et al.*, Metallofiz. Noveish. Tekhnol. **33**, 873 (2011).
13. A.M. Goodman, J. Appl. Phys. **32**, 2550 (1961).
14. V.G. Litovchenko, I.P. Lisovskyy, C. Claeys, V.P. Kladko, S.O. Zlobin, M.V. Muravska, O.O. Efremov, and M.V. Slobodjan, Solid State Phenom. **405**, 131 (2008).
15. O.M. Yefanov and V.P. Kladko, Metallofiz. Noveish. Tekhnol. **28**, 227 (2006).
16. V.B. Molodkin, S.I. Olikhovskii, E.G. Len, E.N. Kislovskii, V.P. Kladko, O.V. Reshetnyk, T.P. Vladimirova, and B.V. Sheludchenko, Phys. Status Solidi A **206**, 1761 (2009).
17. V.P. Kladko, L.I. Datsenko, J. Bak-Misiuk, S.I. Olikhovskii, V.F. Machulin, I.V. Prokopenko, V.B. Molodkin, and Z.V. Maksimenko, J. Phys. D **34**, A87 (2001).
18. V.G. Litovchenko, V.M. Naseka, and A.A. Evtukh, Ukr. Fiz. Zh. **57**, 76 (2012).
19. A. Sarikov, V. Litovchenko, I. Lisovskyy *et al.*, J. Electrochem. Soc. **158**, H772 (2011).

Д.В. Гамов, О.І. Гудименко, В.П. Кладько,
В.Г. Литовченко, В.П. Мельник, О.С. Оберемок,
В.Г. Попов, Ю.О. Поліщук, В.М. Романюк,
В.В. Черненко, В.М. Насека

ДОСЛІДЖЕННЯ РЕКОМБІНАЦІЙНИХ
ХАРАКТЕРИСТИК Cz-КРЕМНІЮ,
ІМПЛАНТОВАНОГО ІОНАМИ ЗАЛІЗА

Р е з ю м е

Проведено порівняльні дослідження процесів дефектоутворення та зміни часу життя неосновних нерівноважних носіїв заряду в кремнії при гетеруванні домішки заліза комбінованим гетером "шар поруватого кремнію + плівка алюмінію". Показано, що в процесі відпалу зразків без гетерного шару в імплантованій області формуються силіцид заліза і дефекти вакансійного типу, внаслідок чого спостерігається сильне зниження часу життя нерівноважних неосновних носіїв заряду. Проведено дослідження впливу гетерного шару на процеси дефектоутворення і перерозподілу атомів заліза, імплантованих в кремній, у випадку їх високих концентрацій в приповерхневій області. Показано, що наявність гетерного шару зменшує ефективність силіцидоутворення в імплантованій області і збільшує концентрацію міжвузлових дефектів в кремнії. Запропоновано фізичну модель процесу гетерування, яка враховує зменшення концентрації атомів заліза в імплантованій області за рахунок гетерування і зменшення концентрації вакансійних дефектів, а також одночасне зростання концентрації дефектів міжвузлового типу, які пов'язані з формуванням комплексів заліза з атомами бору. Саме ці комплекси є рекомбінаційно-активними і не дозволяють відновити час життя носіїв заряду до вихідного значення.